

Slab-wise pulse design enhances the performance of dual source parallel RF transmission at 3T

Xiaoping Wu¹, Dingxin Wang^{1,2}, Jinfeng Tian¹, Sebastian Schmitter¹, Vibhas Deshpande³, Tommy Vaughan¹, Kamil Ugurbil¹, and Pierre-Francois Van de Moortele¹
¹CMRR, Radiology, University of Minnesota, Minneapolis, MN, United States, ²Siemens Medical Solutions USA, Inc., Minneapolis, MN, United States, ³Siemens Medical Solutions USA, Inc., Austin, TX, United States

Introduction: Previous studies have demonstrated that the use of dual source parallel RF transmission (pTx) is advantageous over standard single source RF excitation in 3T body imaging (1-3). In these studies a single RF shim set (i.e., independent RF magnitude and phase modulation upon each of the two transmit channels) was obtained for a multislice sequence to image the entire region of interest (ROI) and therefore the resulting pulses are of suboptimal performance since the full degrees of freedom (DOF's) available in the pulse design are not utilized. Recently, a slab-wise pulse design strategy (4) was introduced to make maximum use of the DOF's in pulse design and was demonstrated capable of providing enhanced RF performance when designing pTx multiband pulses. In this study, we utilize this slab-wise design strategy to evaluate the performance of a 3T birdcage (BC) body coil when operated in the dual transmit mode, and compare it to the conventional single transmit circularly polarized (CP) mode. RF shimming was conducted with local SAR control based on electromagnetic (EM) simulations of the BC coil.

Method: A BC body coil consisting of 32 rungs was modeled using the XFDTD software (Remcom, USA) and was occupied by a human whole body tissue model (Duke, virtual family, 5mm isotropic). EM maps of the coil when operated in the single transmit CP mode were calculated for the entire body by simultaneously driving the two feeding ports with the same RF amplitude but a 90 degree phase difference. The same coil can also be operated in a dual transmit mode in which the two ports are driven independently by a different RF waveform. To design dual transmit pulses, the dual-channel EM maps were simulated by driving only one port at a time. Using the dual transmit mode, RF shimming was conducted to achieve a uniform B1+ distribution within the brain and C-spine area. The ROI was defined within 72 axial tissue slices by excluding air cavities. For slab-wise RF shimming, 12 contiguous axial slabs were prescribed to jointly cover the ROI and a slab-specific RF shim set was calculated for each slab to achieve enhanced RF performance. Because B1+ fields vary relatively slow in space, dual-channel B1+ maps obtained from 24 gapped tissue slices (i.e., 2 slices per slab) were utilized to calculate the RF shim sets rather than considering all 72 tissue slices as B1+ mapping slices. The pulse design was formulated as a local SAR regularized MLS problem (5), $\min_w \|\|Aw\| - 1\|_2^2 + \lambda \sum_{n=1}^{N_{VOP}} \alpha_n \|S_n w\|_2^2$ where A is the transfer matrix involving B1+ maps, w is a vector concatenating the RF shim sets, N_{VOP} is the number of virtual observation points (VOP) (6), S_n is the local SAR matrix derived for the n -th VOP, and α_n is a variable used to reweight the peak local SAR estimate of the n -th VOP. The design problem was solved in a way similar to those in (7). For comparison, another RF shimming was also conducted to only calculate a single RF shim set by treating the entire ROI as a single slab. The L curve quantifying the tradeoff between the peak 10g SAR and excitation errors (defined as the root mean square error (RMSE)) was generated by varying λ in the pulse design. SAR quantities were calculated by exhaustive search assuming single shot EPI with 10° nominal flip angles, 1-mm slice thickness, 1-ms sinc pulse and 1-s TR. All calculations except for EM modeling were performed in Matlab (Mathworks, USA).

Results and Discussion:

Although both dual transmit pulse designs outperformed the single transmit CP mode in terms of B1+ homogenization and SAR reduction, the use of 12 slabs in the pulse design gave rise to more favorable excitation accuracy vs SAR tradeoffs than using a single slab (Fig. 1). The coefficient of variation (CV) of the B1+ distribution within the ROI, calculated as $\text{std}(|B1+|)/\text{mean}(|B1+|)$, was 26% for the single transmit CP mode, and the peak 10 g SAR was 1.5 W/kg. Using the dual transmit mode and choosing the pulse solution near the elbow of the L-curve to provide a favorable balance between the SAR and excitation fidelity, the CV value only reduced to 21% for the single-slab RF shimming and the local SAR reduced by 7% (1.4 vs 1.5 W/kg, Fig. 2). By contrast, the RF shimming using the 12-slab configuration reduced the local SAR by 13% (1.3 vs 1.5 W/kg, Fig. 2), and more importantly, it largely improved the B1+ homogeneity with the CV reduced to 9.8% (Fig. 2). The B1+ discontinuity observed between neighboring slabs can be reduced by either increasing slabs or designing multi-spoke pulses. Although the local SAR to global SAR ratio reduced when using the dual transmit pulses (17 vs 21), it was still far greater than the ratio derived based on the respective SAR limits given by the guideline (i.e. 3.1=10/3.2 in accordance with IEC (8)); this indicates that the local SAR would still be the limiting factor even though it had been explicitly controlled via the pulse design. Note that the same slab-wise RF shim sets can be used in either sequential or simultaneous multislice image acquisitions to achieve an improved RF performance. In summary, we have demonstrated based on EM simulations that dual source pTx in combination with slab-wise RF shimming can significantly improve B1+ homogeneity and reduce local SAR at 3T, and therefore can be used to facilitate a wide array of clinical applications, especially those using a spin echo type sequence where B1+ field homogeneity is critical in attaining high image quality.

References: 1. Willinek et al. Radiology 2010;256(3):966-975. 2. Mueller et al. Radiology 2012;263(1):77-85. 3. Guo et al. JMRI 2013;37(4):875-885. 4. Wu et al. ISMRM2014, p4333. 5. Setsompop et al. MRM 2008;59(4):908-915. 6. Eichfelder et al. MRM 2011;66(5):1468-1476. 7. Lee et al. MRM 2012;67(6):1566-1578. 8. IEC 60601-2-33: ed2010. **Acknowledgments:** P41 EB015894, R21 EB009133, R01 EB006835, and R01 EB007327.

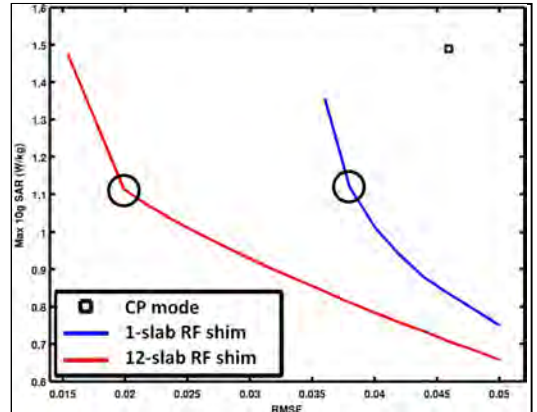


Fig. 1. L curves quantifying tradeoffs between peak 10g SAR and excitation error for RF shimming using a single slab (blue) and 12 slabs (red). The standard single transmit CP mode is marked with a square. The two circles highlight the pulse solutions chosen, for which the SAR and FA maps are shown in Fig. 2.

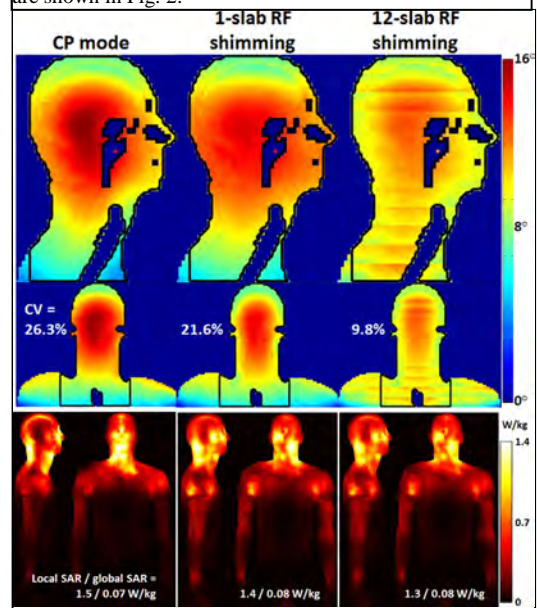


Fig. 2. Flip angle distributions within the head and neck region (top panel) and the maximum intensity projection of corresponding 10-g SAR (bottom panel), for single transmit CP mode (left), 1-slab RF shimming (middle) and 12-slab RF shimming (right). The imaging ROI is marked with black curves. In all cases, the pulse was scaled in amplitude such that the average flip angle in ROI was 10 degrees.